Running on an Incline

J. R. Iversen

T. A. McMahon

Division of Applied Sciences,
Harvard University,
Cambridge, MA 02138

Seven male subjects ran at 3.0 m/s on a motorized treadmill including a force platform under the tread. The subjects ran at each of five treadmill inclinations: +0.17, +0.077, 0, −0.077, and −0.17 radians. The position of the subjects' legs were read from ciné films (100 frames/s). Results of the film and force plate analysis generally corroborated the "hanging triangle" hypothesis, which postulates that the angle between the leg and the vertical upon foot strike does not change as the treadmill is tipped up or down. A mathematical model of running, in which the leg is represented as a nonlinear spring, made satisfactory predictions of the way many parameters of running change with the treadmill angle, including the length of the leg at touchdown and liftoff and the peak leg force in the middle of a step. The peak leg force reaches a maximum at a treadmill angle near −0.12 radians, close to the downhill angle where other authors have found a minimum in the rate of oxygen consumption.

Introduction

As an animal runs, it collides repeatedly with the ground. Running at a steady speed over level ground means that the collisions have a simple consequence: they reverse the animal's downward motion while preserving its forward motion. Our group recently presented a mathematical model of running on the level at steady speed (McMahon and Cheng, 1990). The model was based on the idea that an animal's leg functions as a linear spring. It predicted that although the leg-spring stiffness might be assumed to be fixed, the effective vertical spring stiffness (measured by the slope of a curve plotting vertical force against vertical deflection) increased with running speed. McMahon and Cheng found this prediction and many others concerning the dynamics of running to be in agreement with published observations on running dogs, birds, and humans (Cavagna et al., 1977). The same model was found to give good predictions for the changes in step length, vertical excursions of the center of mass, peak force, and other parameters in experiments in which human runners used an apparatus simulating reduced gravity (He et al., 1991). A conclusion of the latter paper was that the spring stiffness of the leg changes very little across a threefold change in speed and a fivefold change in gravity.

In the studies reported in this paper, human subjects ran on a treadmill that was either level or inclined up or down. The purpose of the work was: 1) to discover experimentally how several important parameters of running change with the angle of the incline, and 2) to see what modifications of the simple model presented by McMahon and Cheng would be sufficient to account for the observed changes in running on an incline. Specifically, we used experimental evidence and a modified version of the McMahon and Cheng model to test the "hanging triangle" hypothesis, which asserts that the angle the leg makes with the vertical upon foot strike does not change as the treadmill is tipped up or down. It was clear at the outset that the McMahon and Cheng model would require at least some modification before it could run uphill or downhill, because it was originally formulated with a linear, conservative leg spring that could neither add to nor subtract from the total energy of the body from step to step.

Contributed by the Bioengineering Division for publication in the JOURNAL OF BIOMECHANICAL ENGINEERING. Manuscript received by the Bioengineering Division January 16, 1991; revised manuscript February 15, 1992. Associate Technical Editor: D. L. Butler.

Methods

Experimental Methods

Apparatus. A motorized treadmill capable of being inclined from 0 to 0.25 radians was modified to include a force platform under the belt. For studies of downhill running, the direction of movement of the belt was reversed. The force platform was 1.2 m long and 0.46 m wide (model OR6-5-1, Advanced Mechanical Technology, Inc., Newton, MA). It had a natural frequency of 160 Hz (measured by striking the unloaded force platform and analyzing the ringing response). The frequency response of the loaded platform was adequate for the purpose, since the force measured normal to the treadmill surface during the running experiments did not include components above 20 Hz in appreciable amplitudes. The treadmill-mounted force platform had been tested and calibrated to prove that it provided an accurate, crosstalk-free measure of the force normal to the treadmill belt during running (Kram and Powell, 1989). In addition to the force measurements, information about the lengths and angles of the subjects' limbs was obtained from sagittal-plane ciné films (Photosonics 1PL camera, Sunnyvale, CA).

Subjects. Seven male subjects, ages 21 through 35, took part in the experiments. All of the subjects were in good physical condition and accustomed to running regularly. Their average body mass was 66.8 (±3.2 s.d.) kg, and their average leg length, measured from the greater trochanter to the floor as the subjects were standing erect, was 0.92 (±0.04 s.d.) m. Because the subjects found it impossible to strike the treadmill

with their heels in uphill running, for consistency the subjects were instructed to run on their forefeet for uphill, level, and downhill running.

Protocols. Each subject ran at one speed (3.0 m/s) at each of five treadmill inclinations: +0.17, +0.077, 0, −0.077, and −0.17 radians. The framing rate of the camera, verified by reference to a 10 rps clock in view of the camera, was 100 frames/s. By reference to the images of a hanging plumb bob for the vertical and a set of marks 1.0 m apart on the treadmill bed, the film record was used to measure the length and angle of the leg from the marked hip point (greater trochanter) to the center of the portion of the foot in contact with the treadmill belt. The angle and length of the leg closest to the camera were read at the moment of touchdown and again at liftoff. Measurements of leg lengths and angles reported here were obtained by averaging 6 strides.

The force record for each steady-state running condition (sampled at 1.0 kHz) was 10 seconds in duration, so that each parameter obtained by a force measurement averages information from approximately 25 foot strikes. The force signal was low-pass filtered (attenuation 12 dB/octave above 50 Hz), then aligned at the beginning of each stance phase to overlay all strikes in order to get one averaged vertical ground reaction force. The displacement normal to the treadmill surface $y(t)$ and the velocity normal to the surface $v(t)$ of the center of mass of a subject were obtained by twice integrating

$$m\,d^2y(t)/dt = f(t) - mg\cos\alpha, \tag{1}$$

where α is the angle of inclination (hill angle), m is the total body mass, $g = 9.81$ m/s^2 is the acceleration due to gravity, and $f(t)$ is the force in the direction normal to the treadmill surface measured by the force platform. Of particular interest were the peak value of the normal force f_{max}, the normal velocity v at touchdown and liftoff, and the normal displacement $y(t)$ throughout the step cycle.

Theoretical Methods

Lumped-Mass Assumption. A fundamental assumption made by McMahon and Cheng (1990) was that the runner's entire body mass could be lumped in a single mass m, and the admittedly complex force-developing properties of the leg, including the actions of all muscles and tendons, could be represented by a single massless, undamped spring (Fig. 1). During the contact phase of a running step, the initial vertical velocity of the mass would be reversed so that the model could rebound upward, the leg could swing forward, and the step cycle could repeat in another identical impact.

Leg-Spring Characteristic. McMahon and Cheng (1990) assumed that the leg was a linear spring of stiffness k_{leg}, and this assumption introduced much symmetry into the solution for a running step. For example, the lengths of the leg at touchdown and liftoff were identical, as were the values of the forward velocity of the mass. The values of the vertical velocity and the leg angle with respect to the vertical were equal and opposite at touchdown and liftoff, and the vertical force and vertical displacement as functions of time were symmetric about their values at mid-step. (In this paper, we shall adhere to the convention that a step refers to the contact period of a single foot while a stride includes the contact periods of both feet plus both aerial periods.)

McMahon and Cheng noted that despite the generally good agreement of their model's predictions with experimental observations on several species of animals, there were some points of disagreement. One of these, noted particularly in the vertical force records of man and kangaroo, was that liftoff was seen to occur when the mass was somewhat higher and the leg was longer than it was on landing. This phenomenon, which we shall call "land short; take off long," is a conspicuous feature of animal locomotion, and had been noted before by other investigators (Cavagna et al., 1977).

Figure 2 shows the force-displacement characteristic of an hypothetical leg spring that has the "land short; take off long" property while still returning, on recoil, all the energy stored within it during compression. In the following, l is the current leg length, l_0 is the fully-extended length of the leg from hip to ground while standing erect, and $l_{touchdown}$ is the leg length at foot strike (generally less than l_0). The spring begins at dimensionless length $L_{touchdown} = l_{touchdown}/l_0$ at zero force. As the spring is compressed, the force rises according to the relation

$$f_{leg}/\mathrm{mg} = K_{shorten}(\Delta L)^n, \tag{2}$$

where n is a constant less than or equal to unity, and

$$\Delta L = (l_{touchdown} - l)/l_0. \tag{3}$$

The parameter $K_{shorten}$ is a dimensionless spring stiffness defined as

Nomenclature

Dimensional parameters (lower case)

- f_{leg} = force acting to compress the leg spring
- f_{vert} = vertical ground reaction force
- f_{max} = maximum value of f_{leg} in a bounce
- g = acceleration due to gravity
- $k_{lengthen}$, $k_{shorten}$ = spring parameters describing the leg (Eqs. (2), (4))
- l = leg length
- $l_{touchdown}$, $l_{liftoff}$ = leg length at touchdown and liftoff
- l_0 = length of the leg from hip to ground while standing erect (uncompressed)
- m = entire body mass, including limbs
- n = leg-spring exponent (Eq. (2))
- t = time
- u = dx/dt = velocity parallel to treadmill belt
- v = dy/dt = velocity normal to treadmill belt
- x = coordinate of the mass in a direction parallel to treadmill belt (Fig. 1)
- y = coordinate of the mass in a direction normal to treadmill belt (Fig. 1)

Dimensionless parameters (upper case)

- $K_{shorten}$ = $k_{shorten}l_0/\mathrm{mg}$, a dimensionless stiffness parameter (Eq. (A.1))
- $K_{lengthen}$ = $k_{lengthen}l_0/\mathrm{mg}$, dimensionless stiffness for lengthening (Eq. (A.2))
- L = l/l_0 = dimensionless leg length
- $L_{touchdown}$, $L_{liftoff}$ = $l_{touchdown}/l_0$, $l_{liftoff}/l_0$
- ΔL = $L_{touchdown} - L$
- T = $t(g/l_0)^{1/2}$ = dimensionless time
- $V_{touchdown}$ = $v/(gl_0)^{1/2}$ at $T = 0$
- $V_{liftoff}$ = $v/(gl_0)^{1/2}$ at the moment the leg force goes to zero (liftoff)
- α = incline of the treadmill (hill angle, Fig. 3)
- $\theta_{touchdown}$, $\theta_{liftoff}$ = angle of the leg at the beginning and end of foot contact (Fig. 3)

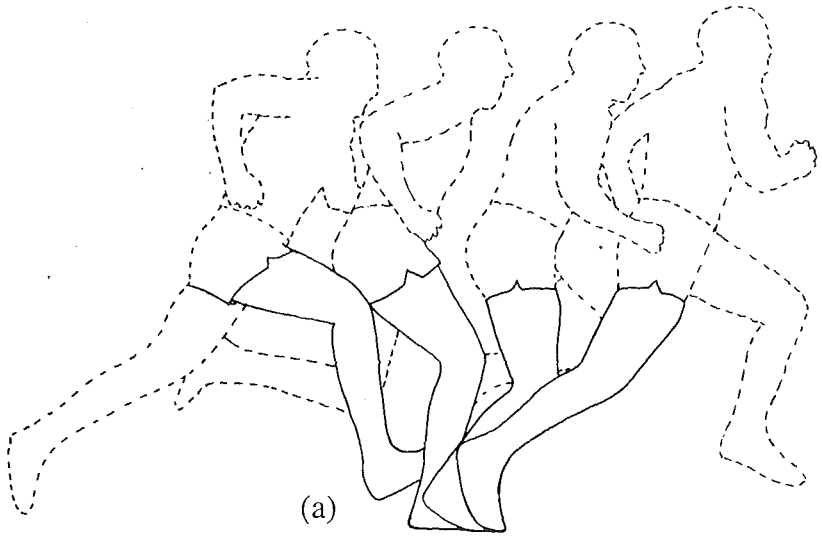

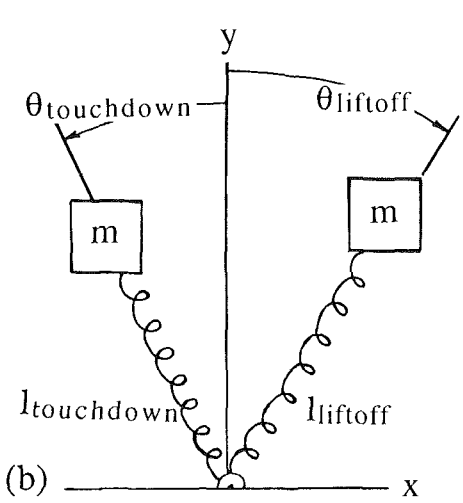

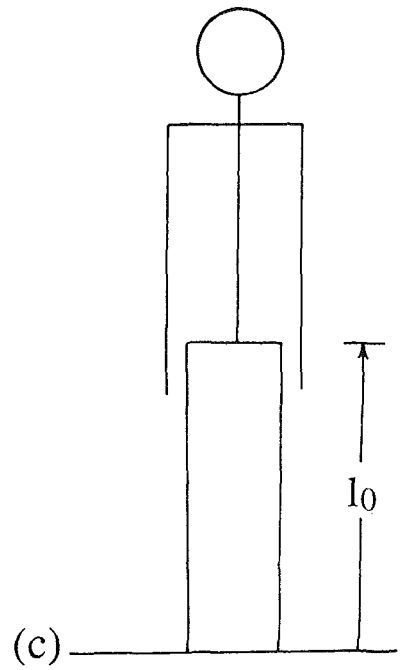

Fig. 1 *(a)* **Tracings of a strobe photograph showing the position of the body at several moments during a contact period for running on the level. *(b)* Schematic diagram of the mathematical model shown at touchdown and at liftoff. The total body mass *m* is assumed to be lumped at the hip. Both the angle of the leg with respect to the vertical and the length of the leg can be greater at liftoff than at touchdown. (c) Schematic showing the fully-extended leg length l_0 measured while standing erect.**

$$K_{\text{shorten}} = k_{\text{shorten}} l_0/\text{mg}, \tag{4}$$

where k_{shorten} is a dimensional parameter numerically equal to the spring stiffness (measured in N/m) of the leg when it has been forced to shorten its entire length ($\Delta L = 1$). The equations describing the motion of the body mass are given in Appendix B. Note that lower-case letters are used for dimensional quantities and upper-case letters for dimensionless parameters. A more complete discussion of the dimensional analysis features underlying the lumped-mass model may be found in McMahon and Cheng (1990).

The assumption will be that any time the leg stops shortening and begins lengthening, it switches to a new, straight characteristic of slope K_{lengthen}. When the model runs uphill, K_{shorten} must be chosen such that the area under the lengthening part of the curve is greater than that under the shortening part. For running downhill, the area under the shortening part must be greater than under the lengthening curve. For running on the level, the areas must be equal, and it is shown in Appendix A that

$$\Delta L_{\text{lengthen}}/\Delta L_{\text{shorten}} = 2/(n+1). \tag{5}$$

For the simulations reported in this paper, n was assigned the value 1/2, for reasons to be explained. Thus, for running on the level, the distance the leg lengthens on recoil is 1/3 greater than the distance it is forced to shorten on compression. As is discussed in Appendix A, it is not necessary for K_{shorten} and K_{lengthen} to be the same for running on the level unless the exponent n is given the value 1.0.

Touchdown Angle: The Hanging Triangle Hypothesis. A schematic diagram depicting the mathematical model running uphill on an inclined treadmill is shown in Fig. 3. The angle of the leg with respect to a perpendicular to the treadmill surface is labelled $\theta_{\text{touchdown}}$; θ_{liftoff} is also marked. (Angles are assumed positive increasing to the right from the normal in this diagram, so θ_{liftoff} is positive and $\theta_{\text{touchdown}}$ is negative.)

We shall assume that the angle the leg makes with the vertical upon touchdown does not change as the treadmill is tipped up or down, and furthermore that the length of the leg when it passes through the vertical position is unchanged by the tread-

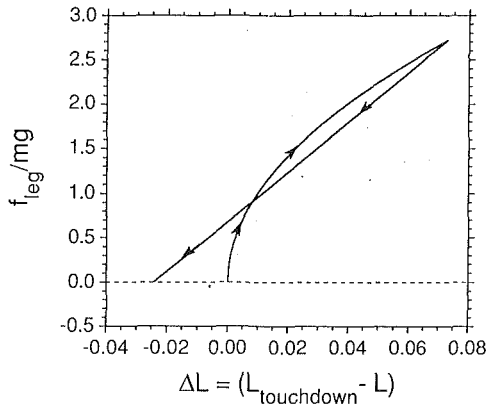

Fig. 2 Nonlinear leg spring characteristic, f_{leg}/mg versus ΔL. This curve comes from a model simulation of running on the level, with $n = 1/2$, $K_{shorten} = 10.079$, and $K_{lengthen} = 28.008$. The arrows indicate the path followed during compression and unloading. The leg is shorter on touchdown than it is on liftoff, demonstrating the "land short, take off long" behavior. Since the characteristic shown is for running on the level, the areas under the shortening and lengthening portions are equal.

mill inclination. These assumptions together will be called the "hanging triangle" hypothesis, in order to evoke the image of a triangle, representing the angular excursion of the leg, hanging by its apex from the hip joint. Humans run with their trunks nearly vertical, whether they are running uphill, on the level, or downhill. Therefore the hanging triangle assumption is roughly equivalent to postulating that the angle of the leg with respect to the trunk at touchdown is independent of the hill angle, perhaps for motor control reasons that depend on afferent input from joint receptors.

Obtaining a Solution. Differential Eqs. (B.2a) and (B.2b) of Appendix B describing the lumped-mass model including the nonlinear leg spring were integrated forward in dimensionless time, and the values for U and V at the end of the flight phase were compared with the starting values. The iterative procedures used to establish values for $K_{lengthen}$ and $K_{shorten}$ for each running condition are explained at the end of Appendix B.

Results

In the remaining sections of this paper, theoretical and experimental results are presented together. This is done for two reasons. First, we wish to use the theory to provide a conceptual framework for relating one experimental finding to another. Second, this method of presentation works well to explain where the inputs to the theoretical model come from.

Specifying the Parameters of the Model. Among the various parameters associated with the model, we chose to regard $\theta_{touchdown}$ and $L_{touchdown}$ as inputs, and required that they be determined by the hanging triangle hypothesis. Another input is the dimensionless forward speed $U_{touchdown} = u/(gl_0)^{1/2}$, which was taken equal to 1.0 in all the simulations, since an average subject running at 3.0 m/s with a leg length of 0.92 m has a value of U equal to 0.999.

The last input the model requires is the dimensionless normal velocity $V_{touchdown} = v/(gl_0)^{1/2}$ at $t = 0$. After trying several alternative assumptions, we elected to rely on the mean value of $V_{touchdown}$ observed in all 7 subjects as an input to our model at each hill angle. In a dynamic sense, taking the value of $V_{touchdown}$ from experimental observations is no different from taking $U_{touchdown}$ from the known treadmill speed. Both $U_{touchdown}$ and $V_{touchdown}$ are required to finish specifying the model for a particular running condition, and both are obtained from experimental measurements. The validity of the model can then be assessed by comparing its predictions with experimental

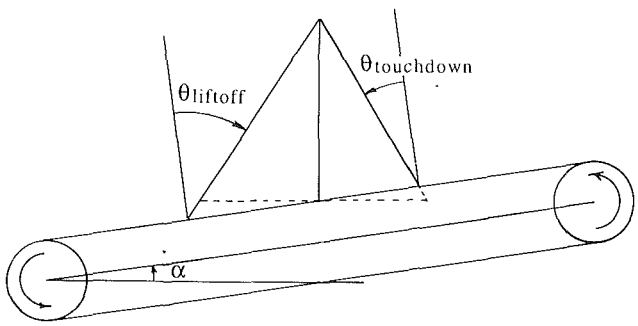

Fig. 3 Diagram showing the hanging triangle construction. The leg-spring model is running uphill on a treadmill tipped up by angle α. The solid lines show the length and angle of the leg at touchdown, again when the leg is vertical, and at liftoff. The broken triangle shows the same measures for running on the level ($\alpha = 0$). The leg length when the leg is vertical is assumed to be independent of hill angle α.

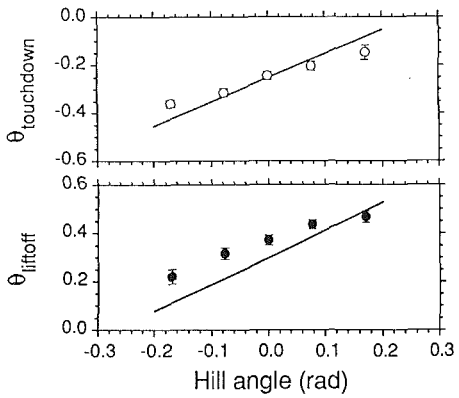

Fig. 4 Leg angle at touchdown (upper plot) and liftoff (lower plot) versus hill angle. Both plots show experimental data (points show the mean of seven subjects; error bars show one standard deviation from the mean) and model predictions (solid curve). $\theta_{touchdown}$ was given as an input to the model and was based on the hanging triangle construction. $\theta_{liftoff}$ was predicted by the model. Positive hill angles are uphill.

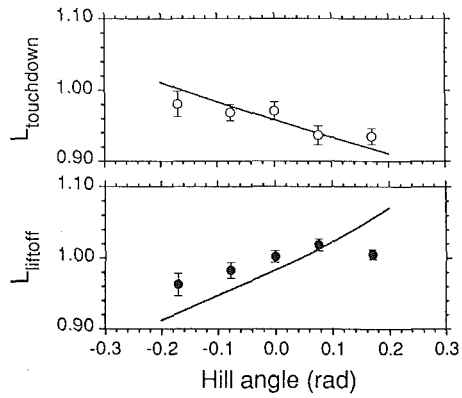

Fig. 5 Dimensionless leg length at touchdown and liftoff versus hill angle. Same format as Fig. 4. $L_{touchdown}$ was an input to the model based on the hanging triangle construction. $L_{liftoff}$ was predicted by the model.

observations that were not used for its specification, including the angle and length of the leg at liftoff, the normal velocity at liftoff, and the normal force applied to the surface of the treadmill. These comparisons are our next subject.

Angles, Lengths, and Velocities. Figures 4, 5 and 6 are each divided into two parts. The curve in the upper portion of each figure shows the input given to the model as a function of treadmill inclination (hill angle). The curve in the lower part of each figure gives the theoretical prediction of the model.

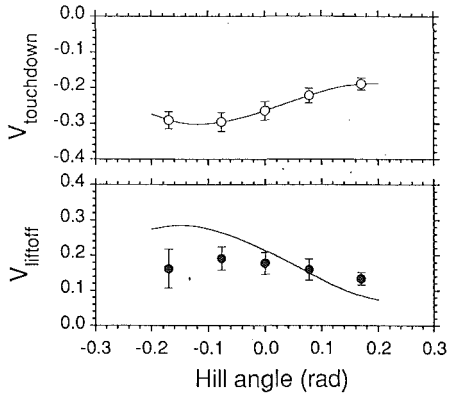

Fig. 6 Dimensionless velocity measured normal to treadmill at touchdown and liftoff versus hill angle. Same format as Fig. 4. $V_{touchdown}$ was an input to the model based on a third order polynomial fit to the experimental data. $V_{liftoff}$ was predicted by the model (curve).

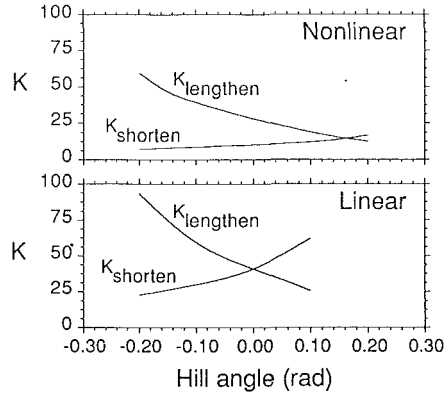

Fig. 8 Dimensionless spring stiffness versus hill angle. Both plots show the values for $K_{shorten}$ and $K_{lengthen}$ which allow the model to run continuously. The upper plot shows the solutions for the nonlinear leg spring model ($n = 1/2$). The lower plot shows the solution for the linear leg spring model. Both models were given the same initial conditions when the foot contacts the ground.

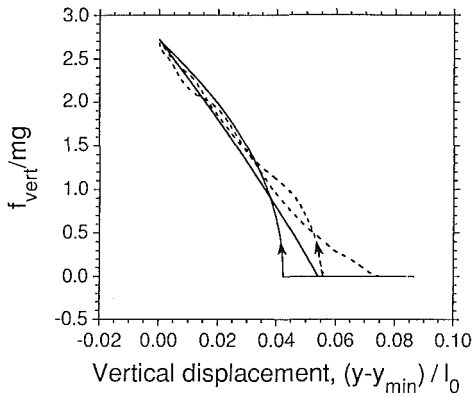

Fig. 7 Dimensionless vertical ground reaction force f_{vert}/mg versus dimensionless vertical displacement $(y - y_{min})/l_0$ for running on the level. Solid line is the model prediction with $n = 1/2$, broken line is experimental data for one subject (average of 25 foot strikes).

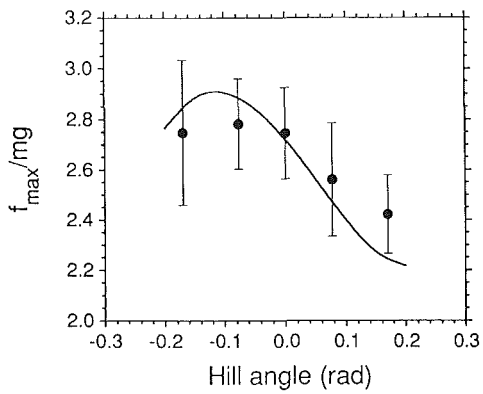

Fig. 9 Dimensionless peak ground reaction force f_{max}/mg measured normal to treadmill versus hill angle. Points show the mean of seven subjects and the error bars show one standard deviation from the mean. The solid curve is the nonlinear leg spring model prediction. Both experimental and predicted values peak near a downhill angle of -0.12 rad.

The points and bars show the means and standard deviations for the 7 subjects at each of the 5 hill angles.

Three observations may be made about these comparisons. 1) The hanging triangle hypothesis is fairly well supported by the measurements of $\theta_{touchdown}$ and $L_{touchdown}$ (open symbols), but in both cases the slope of the solid curve with hill angle is somewhat greater than that shown by the data points. 2) The predicted curves for $\theta_{liftoff}$ and $L_{liftoff}$ (closed symbols) are in reasonable agreement with the trend of the data, with some exceptions. 3) The predicted curve for $V_{liftoff}$ is in poor agreement with the experimental measurements; the data show little variation with hill angle, while the model predicts that V increases as the hill angle decreases, and this trend can be discerned only faintly in the experimental results.

Vertical Force. The dimensionless vertical force f_{vert}/mg is plotted against dimensionless vertical displacement $(y - y_{min})/l_0$ in Fig. 7, which shows theoretical predictions (solid curve) and experimental observations (broken curve) for steady-speed running on the level. The experimental curve was calculated from the average of 25 steps by a single runner. The "land short, take off long" feature appears in both the experimental and theoretical curves. The curves are in better agreement at moderate and high forces than at the low forces reached near touchdown and liftoff. At dimensionless forces above 1.0, both the experimental and theoretical curves show a nearly-linear relationship and low hysteresis.

Spring Parameters. The parameters $K_{lengthen}$ and $K_{shorten}$ which the iterative procedures (Appendix B) gave for each hill angle are shown in the top part of Fig. 8 for the model using the nonlinear leg spring ($n = 1/2$). For comparison, the bottom panel of the figure shows how $K_{lengthen}$ and $K_{shorten}$ are changed when the n in Eq. (2) is given the value unity. Two features are worthy of note. First, both $K_{lengthen}$ and $K_{shorten}$ are larger in the linear than the nonlinear solutions. Second, the curves cross when the hill angle is zero in the linear case but at a large positive (uphill) angle in the nonlinear case.

Peak Normal Force. In Fig. 9, the peak (dimensionless) force normal to the treadmill belt f_{max}/mg is plotted as a function of the hill angle. The theoretical curve has a maximum for downhill running at a hill angle near -0.12 radians. The points show that the experimental maximum occurred near this angle. All the experimental points do not fall precisely on the theoretical curve. However, for each hill angle but the highest uphill incline, the predicted value lies within one standard deviation of the experimental mean, demonstrating that the theory gives a reasonable prediction of the observed trend.

Discussion

Are the Assumptions of the Model Justified? It was necessary to make a number of assumptions to specify the model parameters completely enough to obtain a solution for each

hill angle. Among these were the original lumped-mass assumption for the body, the nonlinear spring assumption for the leg with the further choice of $n = 1/2$, and the hanging-triangle assumption fixing $\theta_{touchdown}$ and $L_{touchdown}$ as a function of hill angle. As discussed above, the initial conditions were completed by using experimental values for the remaining input parameters $U_{touchdown}$ and $V_{touchdown}$.

The generally acceptable agreement between the top panels of Figs. 4 and 5 comparing theory and experiment for $\theta_{touchdown}$ and $L_{touchdown}$ argues for the validity of the hanging triangle hypothesis. The fact that the subjects were instructed to run on the balls of their feet, rather than on their heels, could be expected to add up to 4 cm to the leg length on touchdown (conclusions from direct leg-length measurements), and this may account for some of the variation between the theoretical line and the experimental points in the top panels of Figs. 4 and 5. The agreement in most essential respects between the theoretical and experimental force-displacement curves in Fig. 7 argues for the acceptability of the nonlinear spring characteristic, including the choice $n = 1/2$.

Not all of the predictions of the model were corroborated by the experiments. We have already noted how the expected increase in $V_{liftoff}$ with decreasing hill angle was not observed (Fig. 6, bottom). Furthermore, the predicted $L_{liftoff}$ for the largest hill angle in Fig. 5 was much greater than that measured from the films, perhaps because the model has no physiologically-constrained maximum leg extension, as the human leg does. We tried several alternative sets of assumptions in an effort to improve global agreement between theory and experiment, including different choices for n (1.0, 0.4, 0.25), the assumption that $V_{touchdown}$ did not vary with hill angle, and the input of experimental values for $\theta_{touchdown}$ and $L_{touchdown}$ as well as for $V_{touchdown}$. None of these alternative specifications of the model resulted in an overall improvement between theory and experiment.

We wish to draw special attention to the point that assuming $n = 1$, i.e., a linear spring for both lengthening and shortening, resulted in poorer agreement between theory and experiment with respect to several parameters. The most important disagreement occurred when the $n = 1$ model was used to predict f_{max}/mg as a function of hill angle. For example, at a downhill hill angle of -0.1 radians, the $n = 1$ model predicted that f_{max}/mg would be about 3.6, which is 24 percent higher than the value 2.9 predicted by the $n = 1/2$ specification of the model. Thus, the $n = 1$ model predicted a peak force higher than the measured force by an amount more than 4.5 standard deviations of the nearest experimental point. In addition, the $n = 1$ model predicted that f_{max}/mg would continue to increase as the hill angle decreases, while the $n = 1/2$ model and the experimental results show f_{max}/mg falling for hill angles less than approximately -0.12 radians.

Overall Patterns. A number of patterns may be seen in the experimental observations. Since the theoretical curves most often followed these patterns, the theory may be used as a conceptual framework to recognize a particular pattern.

First, the results of $\theta_{touchdown}$, $\theta_{liftoff}$, $L_{touchdown}$, and $L_{liftoff}$ (Figs. 4 and 5) demonstrate that the hanging triangle hypothesis is a close approximation to what can be observed as humans run uphill and downhill.

Second, the nonlinear leg-spring characteristic (Fig. 2) with $n = 1/2$ gave the best predictions for the various dynamic variables as a function of hill angle, (although not all predictions were within a standard deviation of the experimental mean). It is reasonable to suggest a physiological motivation of the force-extension curve in Fig. 2. Consider that at the moment of touchdown, the knee is partially flexed. When the leg spring is compressed, the muscles acting to extend the knee are forced to lengthen while active. Since a muscle forced to lengthen produces a greater force than the same muscle when it is allowed to shorten, we would expect the lengthening portion of the leg force-extension curve to lie above that of the shortening portion of the curve (Harry et al., 1990). Exceptions to this rule would be expected where the leg shortening velocity was zero (where the lengthening curve joins the shortening curve at peak compression) and also in the left-most portions of the curve when full extension of the knee and plantar flexion of the ankle cause the lengthening leg to reach particularly long lengths. The curves in Fig. 2 have all these properties.

Finally, there is the trend apparent in Fig. 9, where the maximum normal force f_{max}/mg increases as the hill angle decreases, reaching a peak near the downhill angle of -0.12 radians before falling again at steeper downhill angles. Other results (not presented) show that while the contact time is nearly independent of the hill angle in both theory and experiment, the period of the aerial phase rises as the hill angle falls, reaching a peak at an angle near -0.12 radians in both theory and experiment. A simple way of understanding this might be as follows. As the treadmill is tipped down, the body falls farther between steps, and this both takes a longer time and results in a higher $V_{touchdown}$. In order to reverse this higher landing velocity, a stiffer lengthening spring is required, which is the reason why $K_{lengthen}$ increases with decreasing hill angle in Fig. 8. The higher $V_{touchdown}$ and the greater $K_{lengthen}$ give rise to a higher peak leg force as hill angle decreases.

An interesting physiological result which may be relevant to the above discussion concerns steady-state oxygen consumption measurements in humans running on inclined treadmills (Margaria et al., 1963). It was found that the rate of oxygen consumption for running at a fixed speed decreased as the treadmill was tipped down, reaching a minimum when the hill angle was near -0.10 radians, and increasing for more negative angles. The coincidence of this angle with the angle our study found to maximize the normal foot reaction force leads us to speculate that the large forces cause large deformations in elastic elements (perhaps tendons) within the legs. The elastic storage of energy in running has been shown to be associated with reduced metabolic demand in muscle, despite the apparent need to maintain muscle activity to bear the large forces involved (Alexander, 1988; Dawson and Taylor, 1973). Thus running downhill at an angle of about -0.1 radians may be both energetically efficient and particularly punishing to the feet and the leg muscles, all for comprehensible dynamical reasons.

APPENDIX A

A Relation Between $\Delta L_{lengthen}$ and $\Delta L_{shorten}$ for Level Running

Assume that the relation between dimensionless force in the leg spring f_{leg}/mg and dimensionless spring compression ΔL is

$$f_{leg}/mg = K_{shorten}(L_{touchdown} - L)^n \qquad (A.1)$$

when the leg is shortening and

$$f_{leg}/mg = F_{max} - K_{lengthen}(L - L_{min}) \qquad (A.2)$$

when the leg is lengthening. Here, $L_{touchdown} = l_{touchdown}/l_0$ is the dimensionless length of the leg at touchdown, where l_0 is the fully-extended length of the leg from hip to ground when standing erect. Similarly, L_{min} is the dimensionless length of the leg at full compression for a given step cycle and F_{max} is the dimensionless maximum force at full compression. $K_{shorten}$ and $K_{lengthen}$ are dimensionless spring constants of the form $K = kl_0/mg$.

The dimensionless energy stored in the leg as it is compressed from length $L_{touchdown}$ to length L_{min} is

$$\int_0^{\Delta L_{\text{shorten}}} K_{\text{shorten}}(\Delta L)^n d(\Delta L)$$

$$= K_{\text{shorten}}(\Delta L_{\text{shorten}})^{n+1}/(n+1), \quad \text{(A.3)}$$

where

$$\Delta L = L_{\text{touchdown}} - L \quad \text{(A.4)}$$

and the total compression in shortening,

$$\Delta L_{\text{shorten}} = L_{\text{touchdown}} - L_{\min}. \quad \text{(A.5)}$$

The energy released upon extending the leg a distance $\Delta L_{\text{lengthen}} = L_{\text{liftoff}} - L_{\min}$ along the straight line specified by slope K_{lengthen} is

$$K_{\text{lengthen}}(\Delta L_{\text{lengthen}})^2/2. \quad \text{(A.6)}$$

For running on the level, the total energy stored in the spring during shortening must equal the energy released during lengthening. This is the same as setting (A.3) + (A.6) = 0. Solving for $\Delta L_{\text{lengthen}}$ in terms of $\Delta L_{\text{shorten}}$ gives the intermediate result

$$\frac{2}{n+1}\frac{K_{\text{shorten}}}{K_{\text{lengthen}}} = \frac{(\Delta L_{\text{lengthen}})^2}{(\Delta L_{\text{shorten}})^{n+1}}. \quad \text{(A.7)}$$

K_{shorten} and K_{lengthen} may be eliminated from this equation by evaluating Eqs. (A.1) and (A.2) at $L = L_{\min}$ and $L = L_{\text{liftoff}}$, respectively, yielding

$$K_{\text{shorten}} = \frac{F_{\max}}{(\Delta L_{\text{shorten}})^n} \quad \text{(A.8)}$$

and

$$K_{\text{lengthen}} = \frac{F_{\max}}{\Delta L_{\text{lengthen}}} \quad \text{(A.9)}$$

which upon substitution into Eq. (A.7) yields

$$\Delta L_{\text{lengthen}} = [2/(n+1)]\Delta L_{\text{shorten}}. \quad \text{(A.10)}$$

Note that this result is independent of the values used for K_{shorten} and K_{lengthen}, as long as they define an acceptable solution (Appendix B), and does not require that $K_{\text{shorten}} = K_{\text{lengthen}}$.

For $n = 1/2$ as used in the model, (A.10) reduces to

$$\Delta L_{\text{lengthen}} = (4/3)\Delta L_{\text{shorten}}. \quad \text{(A.11)}$$

In the simulation result given in Fig. 2, $\Delta L_{\text{shorten}} = 0.0729$ and $\Delta L_{\text{lengthen}} = 0.0972$. The ratio $\Delta L_{\text{lengthen}}/\Delta L_{\text{shorten}} = 1.333$, which is in agreement with the analytical result from (A.11).

APPENDIX B

The Equations of Motion and Their Solution

Equations of Motion. The dimensional equations of motion of the model center of mass, resolved normal and tangential to the treadmill surface are

$$m\,d^2y/dt^2 = f_{\text{leg}}\cos\theta - \text{mg}\cos\alpha \quad \text{(B.1.a)}$$

$$m\,d^2x/dt^2 = f_{\text{leg}}\sin\theta - \text{mg}\sin\alpha \quad \text{(B.1.b)}$$

where y is the displacement normal to the treadmill belt, x is the displacement tangential to the treadmill surface in the direction of forward motion, α is the tilt angle of the treadmill (see Fig. 3), θ is the angle of the leg measured relative to the treadmill normal (see Figs. 1 and 3), f_{leg} is the force exerted by the leg spring as defined by Eqs. (A.1) and (A.2), m is the body mass, and $g = 9.81$ m/s^2.

Equations (B.1.a) and (B.1.b) may be made dimensionless by dividing both sides by mg and re-expressing in terms of the dimensionless parameters

$$T = t(g/l_0)^{1/2},$$

$$Y = y/l_0,$$

$$X = x/l_0,$$

$$V = dY/dT = v/(gl_0)^{1/2},$$

$$U = dX/dT = u/(gl_0)^{1/2}, \text{ and}$$

$$F_{\text{LEG}} = f_{\text{leg}}/\text{mg},$$

to yield the pair of dimensionless equations of motion

$$d^2Y/dT^2 = F_{\text{LEG}}\cos\theta - \cos\alpha \quad \text{(B.2.a)}$$

$$d^2X/dT^2 = F_{\text{LEG}}\sin\theta - \sin\alpha. \quad \text{(B.2.b)}$$

Iterative Methods. Finding a solution of the model equations for a given set of initial conditions requires identifying the values of K_{shorten} and K_{lengthen} which cause the model to run continuously, that is without changing its trajectory from one step to the next. The following procedure was followed to find a solution for one bounce cycle of the model (contact phase plus air phase) at a given hill angle α:

The initial conditions $U_{\text{touchdown}}$, $V_{\text{touchdown}}$, $\theta_{\text{touchdown}}$, and $L_{\text{touchdown}}$ were set and a starting guess was made for K_{shorten} and K_{lengthen}. The dimensionless Eqs. (B.2.a) and (B.2.b) were integrated forward in dimensionless time by time steps ΔT using a fourth order Runge-Kutta algorithm. The air phase, and thus one bounce cycle, concluded when the mass reached its initial height above the treadmill, for this is where the next contact phase would begin if the leg were reset to its initial angle and length, ready to rebound again.

An acceptable solution was found when the value of U and V at the end of the bounce cycle were within a small tolerance, Δ_{VEL}, of the intial values, $U_{\text{touchdown}}$ and $V_{\text{touchdown}}$. This condition ensures continuous running with no change from one stride to the next. If the pair of K values did not yield an acceptable solution, a new guess was made using the Downhill Simplex Method (Press et al., 1986), operating to minimize a quantity defined as the velocity error,

$$\text{velocity error} = [(U_{\text{end stride}} - U_{\text{touchdown}})^2 + (V_{\text{end stride}} - V_{\text{touchdown}})^2]$$

as a function of K_{shorten} and K_{lengthen}.

All results in this paper were found with $\Delta T = 0.0005$ and $\Delta_{\text{VEL}} = 0.0001$. Decreasing ΔT to one tenth of the value used changed the simulation predictions by less than one hundredth of one percent. Similarly, increasing Δ_{VEL} ten times changed the results by less than one hundredth of one percent.

References

Alexander, R. M., 1988, *Elastic Mechanisms in Animal Movement*, Cambridge University Press, Cambridge, U.K.

Cavagna, G. A., Heglund, N. C., and Taylor, C. R., 1977, "Mechanical Work in Terrestrial Locomotion: Two Basic Mechanisms for Minimizing Energy Expenditure," *Am. J. Physiol.*, Vol. 233, No. 5, pp. R243–R261.

Dawson, T. J., and Taylor, C. R., 1973, "Energetic Cost of Locomotion in Kangaroos," *Nature*, Vol. 246, 5431, pp. 313–314.

Harry, J. D., Ward, A. W., Heglund, N. C., Morgan, D. L., and McMahon, T. A., 1990, "Cross-Bridge Cycling Theories Cannot Explain High-Speed Lengthening Behavior in Frog Muscle," *Biophys. J.*, Vol. 57, pp. 201–208.

He, J., Kram, R., and McMahon, T. A., 1991, "The Mechanics of Running Under Simulated Low Gravity," *J. Appl. Physiol.* Vol. 71, pp. 863–870.

Kram, R., and Powell, A. J., 1989, "A Treadmill-Mounted Force Platform," *J. Appl. Physiol.*, Vol. 67, No. 4, pp. 1692–1698.

Margaria, R., Cerretelli, P., Aghemo, P., and Sassi, G., 1963, "Energy Cost of Running," *J. Appl. Physiol.*, Vol. 18, pp. 367–370.

McMahon, T. A., and Cheng, G. C., 1990, "The Mechanics of Running: How Does Stiffness Couple with Speed?" *J. Biomech.*, Vol. 23, S1, pp. 65–78.

Press, W. H., Flannery, B. P., Teukolsky, S. A., and Vetterling, W. T., 1986, *Numerical Recipes: The Art of Scientific Computing*, Cambridge University Press, New York.